



HAL
open science

**Spectroscopy and efficient laser action under
diode-pumping of a new broadly tunable crystal:
Yb³⁺:Sr₃Y(BO₃)₃**

Sébastien Chenais, Frédéric Druon, François Balembois, Patrick Georges,
Romain Gaume, P.H. Haumesser, Bruno Viana, Gerard Aka, Daniel Vivien

► **To cite this version:**

Sébastien Chenais, Frédéric Druon, François Balembois, Patrick Georges, Romain Gaume, et al.. Spectroscopy and efficient laser action under diode-pumping of a new broadly tunable crystal: Yb³⁺:Sr₃Y(BO₃)₃. Journal of the Optical Society of America B, 2002, 19 (5), pp.1083-1091. hal-00701626

HAL Id: hal-00701626

<https://iogs.hal.science/hal-00701626v1>

Submitted on 25 May 2012

HAL is a multi-disciplinary open access archive for the deposit and dissemination of scientific research documents, whether they are published or not. The documents may come from teaching and research institutions in France or abroad, or from public or private research centers.

L'archive ouverte pluridisciplinaire **HAL**, est destinée au dépôt et à la diffusion de documents scientifiques de niveau recherche, publiés ou non, émanant des établissements d'enseignement et de recherche français ou étrangers, des laboratoires publics ou privés.

Spectroscopy and efficient laser action from diode pumping of a new broadly tunable crystal: $\text{Yb}^{3+}:\text{Sr}_3\text{Y}(\text{BO}_3)_3$

S. Chénaïs, F. Druon, F. Balembois, and P. Georges

Laboratoire Charles Fabry de l'Institut d'Optique, Unité Mixte de Recherche 8501 du Centre National de la Recherche Scientifique, Centre Universitaire, Bât. 503, 91403 Orsay Cedex, France

R. Gaumé, P. H. Haumesser, B. Viana, G. P. Aka, and D. Vivien

Laboratoire de Chimie Appliquée de l'État Solide, Ecole Nationale de Chimie Paris, 11 Rue Pierre et Marie Curie, 75231 Paris Cedex 05, France

Received July 31, 2001; revised manuscript received November 12, 2001

The first demonstration of laser action in a $\text{Yb}^{3+}:\text{Sr}_3\text{Y}(\text{BO}_3)_3$ crystal is reported. This new material exhibits particularly broad absorption and emission bandwidths (6 and 60 nm, respectively) and hence is of particular interest for diode-pumped femtosecond and tunable laser sources. Efficient operation from diode pumping (1.4 W of cw laser power obtained with 3.6 W of diode pump power and as much as 3.4 W of peak power from high-power quasi-cw pumping) together with smooth tunability (over 50 nm FWHM) is reported. For the comparison, efficiency and thermal limitations of Yb:glass and $\text{Yb}:\text{Ca}_4\text{GdO}(\text{BO}_3)_3$ have been investigated under the same conditions. © 2002 Optical Society of America

OCIS codes: 140.5680, 140.3480, 140.3380, 140.6810, 140.3070.

1. INTRODUCTION

The fast development of high-brightness/high-power InGaAs laser diodes used as pump sources within the past decade has led to a strong and still growing interest in Yb-doped materials (crystals, bulk glasses, fibers). Relative to their Nd-doped counterparts, Yb-doped materials are much more likely to yield high efficiencies at high powers.¹ Indeed, the simple electronic structure of Yb^{3+} ions implies the absence of parasitic effects (excited-state absorption or upconversion) and makes high doping rates achievable in most host matrices. In addition, the small quantum defect contributes to weak thermal effects: Yb-doped materials have hence turned out to be useful for efficient high-power cw lasers up to the kilowatt class.² Such lasers are useful for materials processing,³ for example, and, in this field are serious competitors of the widely used Nd:YAG lasers. Scaling toward higher power is limited by thermal problems (fracture, thermal lensing) in the laser medium: High thermal conductivity is therefore desirable. That is why Yb-doped crystals that belong to the family of garnets [such as Yb:YAG (Refs. 1 and 2) and Yb: $\text{Gd}_3\text{Ga}_5\text{O}_{12}$ (Ref. 4)], sesquioxides (Refs. 5 and 6) and, to a lesser extent, tungstates^{7–9} have proved to be promising.

Far from being restricted to the quest for high power, the interest in these materials is also focused on the ability of some Yb^{3+} -doped compounds to exhibit broad absorption and emission bands. We may find several reasons for such behavior. The Yb^{3+} ion exhibits a large overall splitting of its fundamental and excited manifolds, $^2F_{7/2}$ and $^2F_{5/2}$, respectively. For instance, for the Nd^{3+}

ion the overall splitting (ΔE) of the $^4I_{9/2}$ manifold $\Delta E(^4I_{9/2})$ is linked to the overall splitting of the Yb^{31} ion $^2F_{7/2}$ manifold by the rough relationship $\Delta E(^2F_{7/2}) \sim 1.6 \times \Delta E(^4I_{9/2})$.¹⁰ Another specific cause of spectral broadening is electron–phonon interactions between lattice vibrations and electronic levels of the doping ion. These interactions are stronger for Yb^{3+} than for Nd^{3+} for a given host matrix. In addition, such effects as thermal population occupation and host multisite characteristics contribute to inhomogeneous broadening.

Consequently, Yb-doped materials are suitable for a second family of sources that comprises directly diode-pumped femtosecond lasers (oscillators, amplifiers) and tunable lasers in the near infrared (1000–1100 nm). The various applications of diode-pumped femtosecond lasers, and their numerous advantages compared with conventional Ti:sapphire lasers, have already been discussed extensively elsewhere. For these applications several materials, in particular, borates [$\text{Ca}_4\text{GdO}(\text{BO}_3)_3$ (GdCOB; Ref. 11) and $\text{Ca}_4\text{YO}(\text{BO}_3)_3$ (Ref. 12)], silicates,^{10,13} tungstates [$\text{KY}(\text{WO}_4)_2$ and $\text{KGd}(\text{WO}_4)_2$ (Ref. 14)], and glasses,¹⁵ are important. For all these materials, the common characteristic is a broad fluorescence spectrum.

Achieving such a broad spectrum requires that the Yb^{3+} ions experience a high degree of structural disorder, so discrete energy levels tend to average in a smooth, broad spectrum. This averaging occurs straightforwardly in glasses in which there is no crystalline structure. The emission spectrum of an Yb-doped glass is typically 35–60 nm wide and is remarkably smooth [see Fig. 1(b)]. To exploit this broad spectrum, diode-pumped

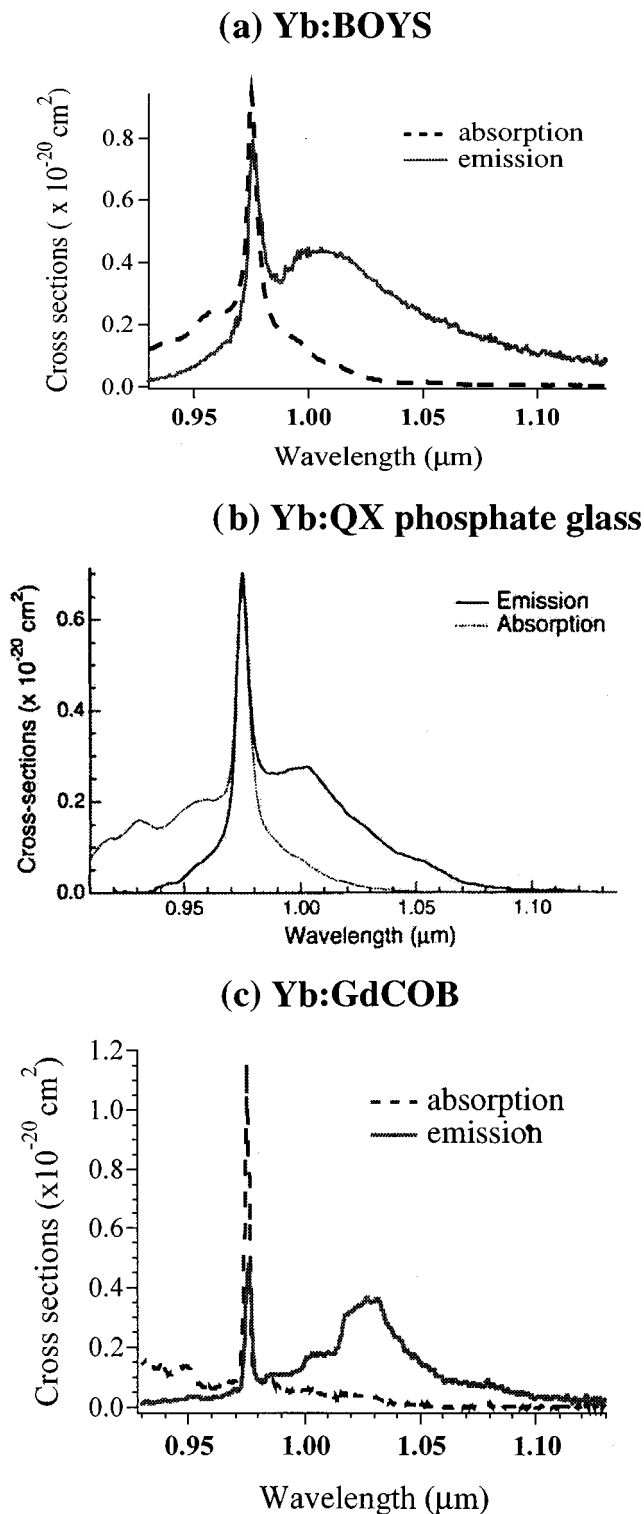


Fig. 1. Absorption and emission spectra of Yb:BOYS, Yb:glass, and Yb:GdCOB. (a) Measured absorption and emission cross sections of BOYS doped with 20-at. % Yb_2O_3 (π polarization). (b) Absorption and emission cross sections of a Kigre QX phosphate glass doped with 15-at. % Yb_2O_3 (from Ref. 15). (c) Absorption (for $E//Y$) and emission (for $E//Z$) cross sections of GdCOB doped with 15-at. % Yb_2O_3 .

femtosecond oscillators with bulk Yb-doped glasses were built; 58-fs pulses hence were obtained from an Yb-doped phosphate glass (QX from Kigre, Inc.) oscillator.¹⁵

However, glasses have low emission cross sections, low radiative lifetimes, and bad thermal conductivity (see the data for QX phosphate glass in Table 1); all these properties result from a lack of microscopic order. Laser efficiencies are usually low,^{15,17} and complex pumping strategies must be used to overcome thermal issues and reach average powers up to the watt level.¹⁸ In contrast, crystals are well known for their much better spectroscopic and thermal properties, which lead to high laser efficiencies even at high powers. But the crystalline structure tends also to keep the emission and absorption bands narrow (the emission bandwidth is only 10-nm broad in Yb:YAG, for example).

A perfect material for generation of ultrashort pulses and efficient tunable lasers will therefore be a crystal with good spectroscopic properties and high thermal conductivity, together with a glasslike emission spectrum. In other words, the material should combine the good qualities of both crystals and glasses.

A promising candidate for bridging the gap between crystals and glasses is Yb:GdCOB. Recently, efficient tunable laser action in this crystal was reported: 3.2 W of power, cw, was obtained from pumping with a 10-W laser diode emitting at 976 nm, and the laser was continuously tunable from 1018 to 1086 nm. Mode locking of this laser was also demonstrated, with low-power high-brightness pumping (2 W from a single-stripe $1 \times 100 \mu\text{m}$ emitter), leading to 90-fs pulses.¹⁹ Tungstates [$\text{Yb:KLn}(\text{WO}_4)_2$, where Ln is Gd or Y] are also valuable crystals: Efficient cw operation (1.3 W for 4 W of incident power) in Yb:KGd(WO_4)₂ with a wavelength tunability within a 22-nm range was recently reported.¹⁴ Although the emission spectrum is narrower than those of borates, pulse durations as short as 71 fs were reported with Yb:KY(WO_4)₂.²⁰

Here we describe the performance and tunability of a new crystal, $\text{Yb}^{3+}:\text{Sr}_3\text{Y}(\text{BO}_3)_3$ (Yb:BOYS), diode pumped in the quasi-cw and cw regimes. Performance and thermal limitations are compared experimentally, under the same conditions, with those of Yb:GdCOB and Yb:QX phosphate glass that are clearly intended for the same applications.

2. SPECTROSCOPY OF $\text{Yb}^{3+}:\text{Sr}_3\text{Y}(\text{BO}_3)_3$

Yb:BOYS melts congruently at a fairly low temperature (1400 °C), making its growth by the Czochralski process easy. Boules with high optical quality and large dimensions have been grown by this technique (see Fig. 2). The structural characteristics of $\text{Sr}_3\text{Y}(\text{BO}_3)_3$ were described elsewhere.^{13,21} Ytterbium ions can substitute for yttrium ions of the structure because they have similar ionic radii; hence solid solutions of $\text{Sr}_3(\text{Y}_{1-x}\text{Yb}_x)(\text{BO}_3)_3$ with substitution rates ranging from $x = 0$ to $x = 1$ can be obtained without affecting the crystal quality. In the present paper we discuss laser characterizations of 20 at. % Yb^{3+} -doped crystals (that is, $x = 0.2$), corresponding to a concentration of 9.6×10^{20} ions/ cm^3 . As far their optical properties are concerned, these crystals are uniaxial crystals whose optic axes (c -crystallographic axes) will be colinear to the direction of light propagation ($k//c$).

The absorption and emission spectra at room temperature are shown in Fig. 1(a) for π polarization. The spectra for σ polarization are not given because we did not notice any measurable difference between the π and σ -polarization spectra. For comparison we also show the absorption and emission spectra of 15-at.-%-doped QX phosphate glass [Fig. 1(b)], and 15-at.-%-doped GdCOB [Fig. 1(c)]. For the latter crystal the absorption is given for an electric field $E//Y$, and the emission is given for $E//Z$.¹⁶ The similarity of the absorption and emission spectra of Yb:BOYS to those of Yb:glass is clearly remarkable. The Yb:BOYS crystal turns out to have in addition a broader spectrum than the phosphate glass (60 compared with 35 nm). Note that, because of the large broadening of these spectra, it is hazardous to measure an emission bandwidth by use of the common criterion of FWHM on the emission spectrum because the FWHM spectrum largely overlaps the absorption spectrum. To overcome this ambiguity we measured the emission bandwidths listed in Table 1 FWHM on the gain cross-

section spectrum for a fractional excited-state population $\beta = 0.5$. We chose QX phosphate glass rather than other glasses for the following comparative tests by drawing on the results of Hönninger *et al.*¹⁵ They pointed out that QX phosphate glass yields better efficiency and shorter pulses (when the glass is used in femtosecond oscillators) than silicate (Q-246) or fluorophosphate glasses.

In addition, Yb:BOYS has a broader but, interestingly, a smoother spectrum than Yb:GdCOB. It was previously shown that the broad absorption and emission bands of Yb:BOYS are linked to vibronic transitions and multisite behavior.¹³ Moreover, the Yb³⁺ ions have a strong crystal field within the lattice (the ${}^2F_{7/2}$ splitting of Yb³⁺ is approximately 800 cm⁻¹), which should lead to a small lower-laser-level thermal population and to reduced reabsorption losses. The spectroscopic and thermal properties of Yb:BOYS are summarized in Table 1.

To complete our spectroscopic characterizations we carried out fluorescence decay measurements at room tem-

Table 1. Spectroscopic and Thermal Properties of Yb:BOYS and of Several Yb-Doped Tunable Materials

Property	Material				
	Yb:BOYS	Yb:Phosphate Glass QX	Yb:GdCOB	Yb:YAG	Yb:KG d(WO ₄) ₂
Zero-line absorption wavelength (nm)	975	975	976	968	981
Absorption linewidth (nm, FWHM) ^a	6	7	3	3	3.5
Fluorescence lifetime (ms)	1.1	1.3	2.6	0.95	0.75
Typically observed lasing wavelength (nm)	1066	1054	1043	1030	1026
Emission cross section at typical laser wavelength ($\times 10^{-20}$ cm ²)	0.2	0.05	0.35	2.2	2.8
Emission bandwidth (nm) ^b	60	35	50	10	20
Thermal conductivity (W m ⁻¹ K ⁻¹) ^c	1.8	0.85	2.1	14	3.3
Reference	13 and this work	15	11	15, 16	7, 8

^a At the zero-line wavelength.

^b Measured FWHM on the gain cross-section spectrum for a fractional excited-state population $\beta = 0.5$.

^c For undoped crystals. When the conductivity is different along the crystallographic axes the average value is given.

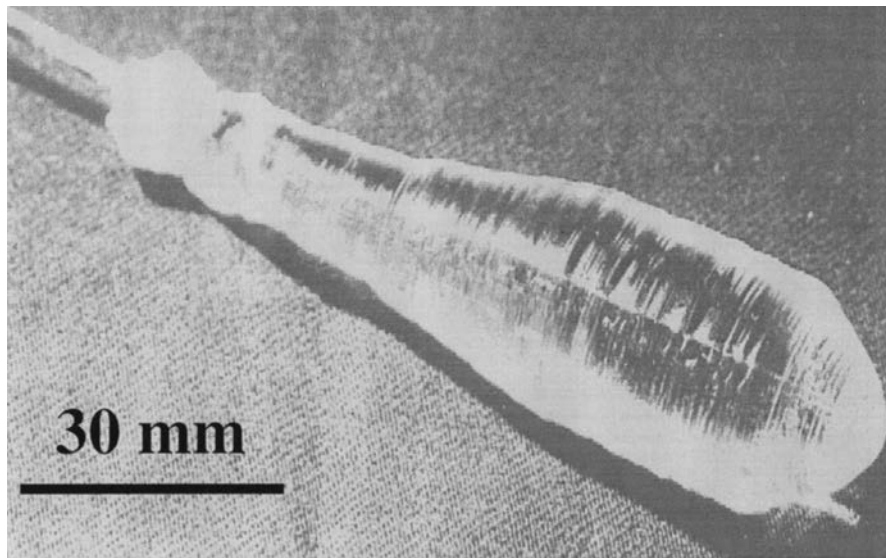


Fig. 2. Single Yb:BOYS crystal.

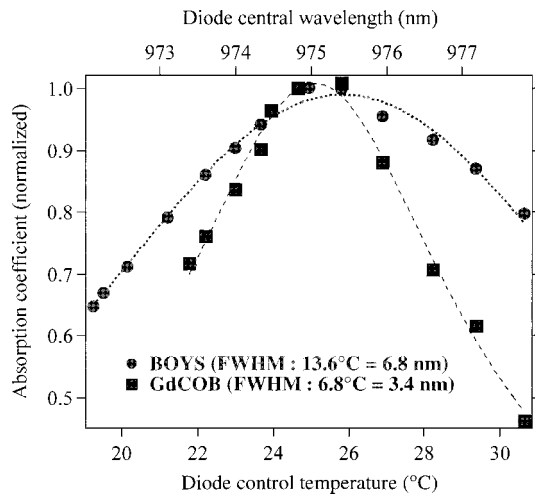


Fig. 3. Absorption versus diode temperature for Yb:BOYS and Yb:GdCOB.

perature on single crystals grown by the Czochralski method. It appears that the measured lifetime τ_{exp} is strongly dependent on the ytterbium concentration. It increases from 1.2 ms for diluted samples (0.5-at. % Yb-doped) to 2.4 ms for 15-at. % Yb-doped BOYS. The increase of experimental lifetime with ytterbium concentration is evidence of a strong reabsorption process, enhanced by the fact that the measurements were carried out with bulk crystals. In addition, the measured lifetime at low concentration is in good agreement with the calculated radiative lifetimes $\tau_{\text{rad}} = 1.1$ ms obtained from the absorption spectrum.

An interesting property of Yb:BOYS is its broad absorption peak at 975 nm, approximately 6 nm, which makes spectral linewidth specifications of laser diodes less demanding. In Yb-doped materials this absorption line, known as the zero line, is usually narrower (3 nm FWHM for YAG and GdCOB, for example): Given that the spectrum of high-power diodes is typically 3 nm broad (even more for diodes emitting more than roughly 10 W), this is a significant drawback for diode pumping. The wider absorption bandwidth of Yb:BOYS means that the laser output power is less sensitive to drift of the diode pump wavelength caused by changes in temperature or by aging. It may also make easier the use of pump diodes operating in the quasi-cw regime without significant reduction of the absorption efficiency as a result of spectral shifting.

We carried out a simple experiment to compare the absorption sensitivity to diode spectral shifts of Yb:BOYS with that of Yb:GdCOB. The absorption coefficient per unit length was measured relative to the diode temperature for a given injected current that corresponded to an output power of approximately 10 W (at this output level the spectral linewidth of the diode is 3 nm FWHM). We did not focus the diode beam onto the crystal so we could measure the absorption without bleaching and prevent thermal effects or fracture. Results are shown in Fig. 3: It appears that the temperature range beyond which the absorption is reduced by a factor of 2 is close to 13 °C for Yb:BOYS and 7 °C for Yb:GdCOB. Given that the central emission wavelength scales linearly with tempera-

ture, with a measured slope of 0.5 nm/°C, these temperature ranges correspond, in terms of wavelength drift, to 6.8 and 3.4 nm, respectively. These measured ranges are in agreement with spectroscopic data, as the absorption linewidth is 6 nm (FWHM) for BOYS and 3 nm (FWHM) for GdCOB.

3. COMPARISON OF THE PERFORMANCE OF QUASI-CW-PUMPED Yb:BOYS, Yb:GdCOB, AND Yb:QX PHOSPHATE GLASS UNDER THE SAME CONDITIONS

A. Experimental Setup

The laser experiments were performed with a high-brightness beam-shaped laser diode (OPC-D010-976-HB250, OptoPower, Inc.) as the pump source, emitting 10 W of power at 975 nm (see Fig. 4). The diode was designed primarily to be coupled in a fiber with a core diameter of 250 μm , but, owing to alteration of the fiber, we collected the beam directly after the beam-shaping optics. The diode beam was imaged upon the crystal by two 60-nm focal-length doublets that were antireflection coated at 980 nm on both faces. At the crystal location we measured a 180 $\mu\text{m} \times 235 \mu\text{m}$ spot size (see the beam pattern in Fig. 4), nearly Gaussian shaped in both directions in the far field with full-angle divergences of 15.6° in the horizontal and 13.4° in the vertical directions; the junction plane of the diode was horizontal. These divergence values are, respectively, 39 and 43 times greater than those of a diffraction-limited Gaussian beam with the same spot size.

The cavity was a V-type three-mirror resonator. The back mirror was a plane dichroic mirror that had been high-reflection coated over 1020–1200 nm on the rear face, and antireflection coated for the pump wavelength on both faces. The folding mirror was a concave meniscus (radius of curvature $R = 100$ mm; high-reflection coated over 1020–1200 nm and also antireflection coated for the pump wavelength on both faces to prevent detrimental feedback into the diode). The third mirror was a flat output coupler.

The path lengths between the rear mirror and the folding mirror and between the folding mirror and the output coupler were, respectively, 80 and 85 mm, permitting single-transverse-mode operation. In addition, we ac-

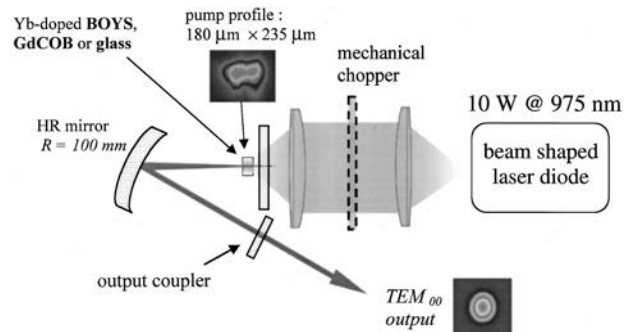


Fig. 4. Experimental setup for high-power laser characterizations of Yb:BOYS, Yb:GdCOB, and Yb:QX phosphate glass. HR, highly reflective.

Table 2. Properties of the Crystals and Glasses Used for Laser Tests

Property	Material		
	Yb:BOYS	Yb:Phosphate Glass QX	Yb:GdCOB
Doping level (at. % Yb ³⁺)	20	15	15
Ion doping density ($\times 10^{20}$ cm ⁻³)	9.6	≈ 20	6.6
Index of refraction	1.74	1.535 ^b	1.70
Length (mm)	2.38	2.52	2.89
Transverse section (mm \times mm)	4 \times 4	5 \times 5	5 \times 5
Orientation	<i>k</i> // <i>c</i> (propagation along optic axis)	Isotropic	<i>k</i> // <i>Y</i> ^c

^a All crystals were antireflection coated on both faces.

^b Ref. 15.

^c *Y* is a crystallophysic axis (see Ref. 16).

counted for the foreseen variations in the cavity spot size caused by thermal lensing by choosing a resonator design in which the cavity spot size increases slightly with the dioptric power of the thermally induced lens in accordance with an argument raised by Clarkson *et al.*²² Single-transverse-mode operation was hence maintained even for strong thermal lenses. The cavity-to-pump spot size ratio was approximately 1 without thermal lensing and 1.1 for a thermal lens focal length of 50 mm, which is the order of magnitude observed for thermal lenses in Yb:GdCOB.¹¹

For a comparative study we used samples of Yb:BOYS, Yb:GdCOB, and Yb:QX phosphate glass whose properties (dimensions, doping level, orientation) are summarized in Table 2. These crystals or glasses were wrapped with indium foil and clamped in a water-cooled copper block. The water temperature was maintained at 15 °C.

To study independently the influence on performance of spectroscopic properties on the one hand, and of thermal properties on the other hand, we first measured the laser efficiencies with a mechanical chopper inserted between the two doublets. This chopper allowed us to keep the same pump peak power but with a reduced thermal load. We first used a 1/17 duty cycle; the dependence of laser power on the duty cycle (from 1/17 to the cw regime) is investigated in Section 4 below.

B. Experimental Procedure for Comparative Tests

We took care to pump the crystals under the same conditions. By “same conditions” we mean that the same pumping configuration and the same way of evacuating heat from the crystals (or glasses) were used. Given this starting point, we then optimized the output power for each material. In addition, the following important precautions were fulfilled:

(1) The absorbed pump power under lasing conditions was as far as possible the same for all crystals tested. As a result of reabsorption losses in the noninverted regions of the pumped volume, the optimum absorbed fraction was less than 100%, typically $\sim 70\%$, which enabled us to choose the crystal length. But, owing to the absorption saturation and gain saturation that occur at high pumping intensities, foreseeing the absorption (under lasing conditions) is not a straightforward matter. Because all the crystals do not absorb exactly the same fraction of the incident pump power, and because the diode wavelength

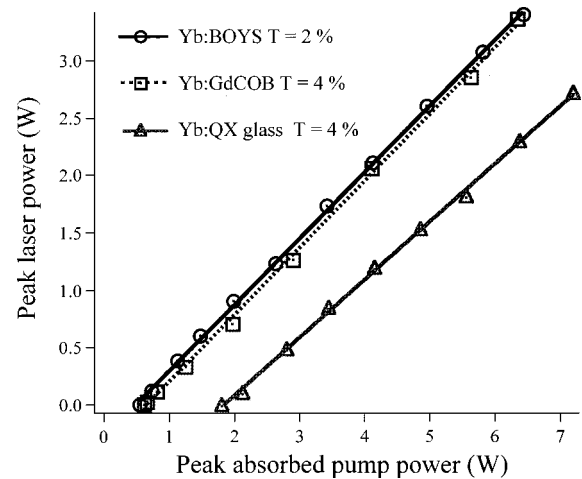


Fig. 5. Efficiency of Yb:BOYS, Yb:GdCOB, and Yb:glass in the quasi-cw regime (chopping duty cycle: 1/17). *T* is the optimal output coupler transmission.

shifts when the pump current is increased, we measured the output laser power as a function of the absorbed pump power under lasing conditions.

(2) In most applications, not only high power but also high beam quality are required. That is why we carried out the following comparisons with the resonator described in Subsection 3.A such that the laser was always operated in a TEM₀₀ single transverse mode.

(3) We experimentally selected the output coupler that led to the highest output power (among a set of available transmission coefficients ranging from 0.5% to 50%).

(4) The crystals and glasses used in these tests had excellent optical quality. For a reliable comparison, the internal losses of the compared materials must indeed be negligible, or at least comparable. One can separate three causes of loss in Yb-doped materials, as follows: (1) The laser beam reabsorption that is due to the thermal population of the lower level of the laser transition. [These losses depend on the material as well as on the pumping arrangement (by means of absorption saturation). They contribute to determination of the lasing wavelength. They can vary from one material to another but are an integral part of the laser test because they depend only on the material under the same pumping conditions]; (2) The scattering losses, which in our case were negligible in all the tested materials because no inclu-

sions or microbubbles were detectable in the samples as observed between crossed polarizers with a microscope; and (3) the losses caused by quenching of the excited-state population by traces of impurities such as thulium and erbium. In the three tested materials compared here, none of these ions could be detected by selective excitation with a tunable Ti:sapphire laser. We thus came to the conclusion that internal losses were negligible.

C. Compared Efficiencies

Comparison for chopped pumping (duty cycle: 1/17), that is, negligible thermal loading, leads to the results summarized in Fig. 5 and Table 3. We obtained 3.4 W of peak power for 6.4 W of absorbed pump power, with a threshold of 550 mW and a slope efficiency of 56% (with respect to the absorbed pump power under lasing conditions). The optimum transmission coefficient for the output coupler was experimentally found to be 2%. For this coupler the lasing wavelength was 1066 nm. Note that, because of reabsorption, the wavelength was smaller for higher-transmission coefficients. The performance of Yb:GdCOB under the same conditions (see Subsection 3.B for details) is substantially the same (Table 2). However, Yb:glass is less efficient, with a higher threshold (1.8 W) and a slightly lower slope efficiency. At this step of comparison it is clear that Yb:BOYS is, without consideration of thermal issues at this stage, more efficient than glass and as efficient as Yb:GdCOB.

D. Compared Wavelength Tuning Ranges

We tuned the laser wavelength by inserting a dispersive SF6 prism into the cavity. The prism was cut symmetrically such that the incident and emergent beams struck the prism at the Brewster angle. The prism thus provided minimum losses for TM polarization when it was inserted into the cavity. Because the uniaxial Yb:BOYS crystal was cut along its optic axis, and because Yb:glass is isotropic, the output from these lasers (without a prism inside the cavity) was not polarized. In contrast, Yb:GdCOB is a biaxial crystal; the orientation was therefore chosen such that the polarized lasing mode matched the TM polarization with respect to the prism surface, that is, with the electric field horizontal. Tuning curves, obtained under the same conditions for Yb:BOYS, Yb:GdCOB, and Yb:glass, are shown in Fig. 6. The tuning range is limited to the smaller wavelengths by the

mirror coatings and also by reabsorption losses owing to thermal population of the lower laser level. Conversely, it is limited to the longer wavelengths only by the available gain in the laser medium. The total extent of the tuning range is therefore not a pertinent characterization of a given material; but one can notice that the shape of the measured tuning curves is linked to the shape of the emission spectrum. Although some authors have shown tuning curves that are broader than emission spectra and somewhat different in shape, for example, in Yb:YAG pumped with a thin-disk architecture,²³ the main features of the spectrum—width, presence of peaks at given wavelengths—are always recognizable in the tuning curve. In our case, continuous and smooth tunability was achieved with Yb:BOYS from 1017 to 1086 nm. A comparable shape was obtained for Yb:glass, consistently with the similarity pointed out for the emission spectra. However, glass is tunable only to 1066 nm because of its low gain and narrower spectrum. The measured shape is consistent with results obtained by Danger *et al.* with different glasses.¹⁷ By contrast, whereas Yb:GdCOB is as tunable as Yb:BOYS in terms of total tuning range (which spreads from 1018 to 1086 nm), its shape is not so smooth and regular.

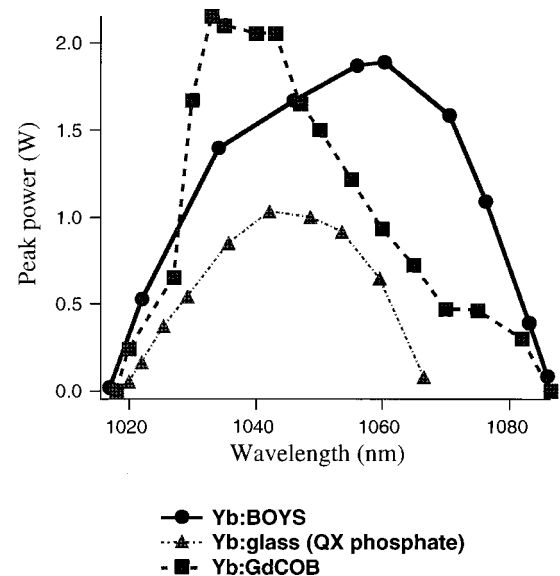


Fig. 6. Tuning curves of Yb:BOYS, Yb:GdCOB, and Yb:glass obtained under the same experimental conditions.

Table 3. Comparison of the Performance of Quasi-CW-Pumped Yb:BOYS, Yb:GdCOB, and Yb:Glass^a

Property	Material		
	Yb:BOYS	Yb:GdCOB	Yb:Phosphate QX
Peak output power (W)	3.4	3.4	2.7
Slope efficiency (%)	56.1	58.3	50.4
Absorbed peak power at threshold	550 mW	700 mW	1.8 W
Optimum output coupler transmission (%)	2	4	4
Observed laser wavelength (nm)	1066	1043	1054
Tunability (nm, FWHM)	50	30	34

^aDuty cycle: 1/17.

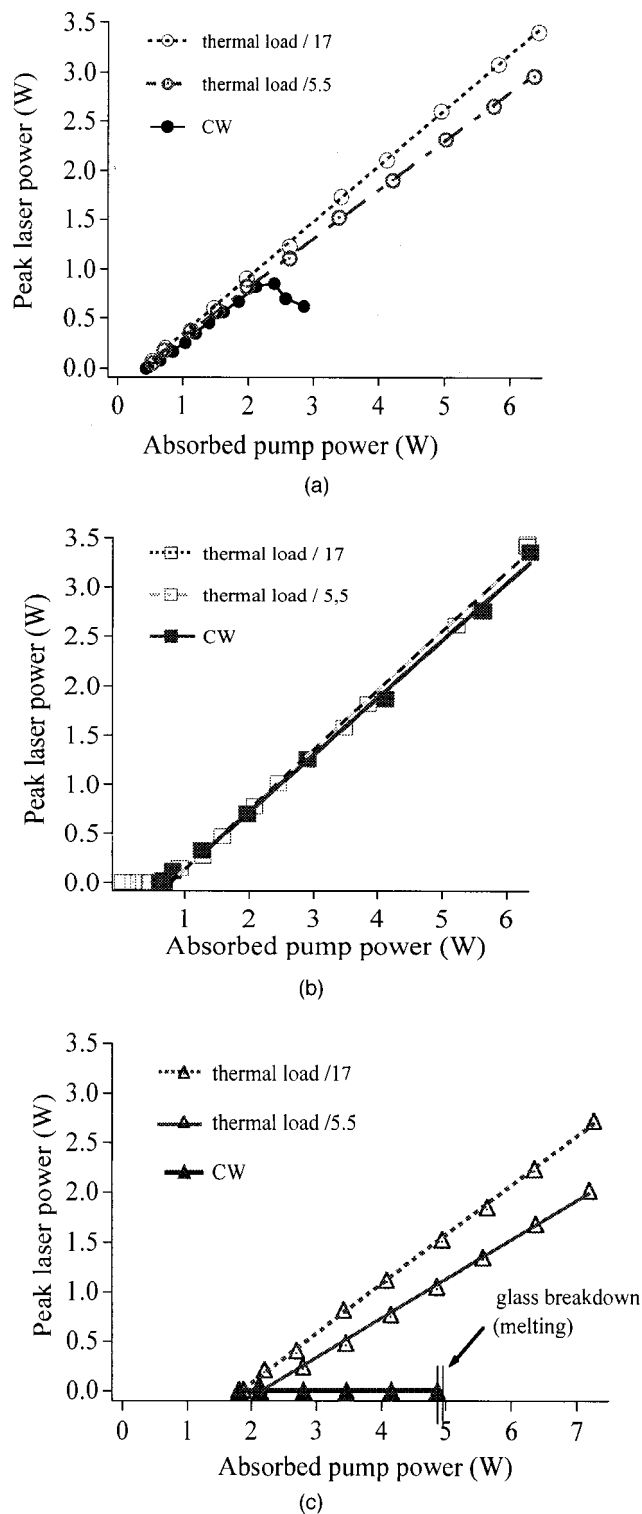


Fig. 7. Performance for quasi-cw and cw pumping of (a) Yb:BOYS, (b) Yb:GdCOB, and (c) Yb:QX phosphate glass.

4. THERMAL LIMITATIONS

To investigate the influence of thermal effects on laser performance we carried out the same comparative tests for various duty cycles of the chopped pump beam: 1/17,

1/5.5, and cw operation. Results are shown in Fig. 7. For Yb:BOYS [Fig. 7(a)] the slope efficiency is slightly less for 1/5.5 chopped pumping (by a factor of 13% with respect to the slope efficiency measured with the 1/17 duty cycle). In cw operation, roll-off appears from 2.2 W of absorbed pump power (5 W of incident diode power): The output power then decreases, proving that thermal effects are detrimental to performance. When the diode power is set to its maximum value (10 W), the crystal undergoes fracture. A way to shift the roll-off value to a higher level might be the use of smaller crystals or of other pumping strategies such as thin-disk geometry.

Conversely, no thermal limitations were found under the same conditions for Yb:GdCOB; the efficiency remained the same, whatever the duty cycle, as shown in Fig. 7(b). The situation was radically different for Yb:QX phosphate glass: Not only did the slope efficiency drop by 18% between the 1/17 and the 1/5.5 duty cycles but no laser oscillation could be obtained any more in the cw regime [Fig. 7(c)]. Indeed, from 4.8 W of absorbed power, the glass sample undergoes melting at the focal point of the laser diode. Thus, as far as withstanding high-power operation is concerned, Yb:BOYS outperforms Yb:glass but is less efficient than Yb:GdCOB.

5. CW OPERATION WITH LOW-POWER-HIGH-BRIGHTNESS DIODE PUMPING

At this step of the study it is clear that Yb:BOYS exhibits good efficiency at low average pump powers that is comparable with Yb:GdCOB, along with easier tunability, but is not well suited for high-power applications. The most clearly foreseeable application for this new crystal is therefore in the field of low-average-power oscillators. We thus pumped the crystal with laser diodes of lower power but higher brightness. The setup used in this final experiment is shown in Fig. 8. Two single-stripe diodes located at opposite sides of the crystal were used as the pump sources. The first diode (Diode #1) is a $1 \mu\text{m} \times 100 \mu\text{m}$ single-stripe emitter producing 1.6 W of power at 975 nm, followed by an anamorphic imaging system, so we obtained 1.1 W incident onto the crystal. The second diode (Diode #2) is a 2-W $1 \mu\text{m} \times 100 \mu\text{m}$ single-stripe diode at 975 nm and yielded 1.4 W of power incident onto the crystal. The resonator design is that described in Subsection 3.A. The efficiency of the laser when only Diode #1 was turned on is shown in Fig. 9: We obtained 450 mW of power (in a diffraction-limited beam) for a 4% output coupler. The slope efficiency with respect to the absorbed pump power was 76.5% in this case (the theoretical value as a result of the quantum defect is 91%), and the threshold was 375 mW. When Diode #2 was turned on in addition, the output power reached 1.4 W (always in a diffraction-limited beam) for a total of 2.5 W of incident power. With this setup we thus obtained a laser-to-diode power conversion efficiency of 39%, which is slightly higher than the 34% conversion efficiency obtained in the quasi-cw regime (cf. Table 3) with lower brightness pumping.

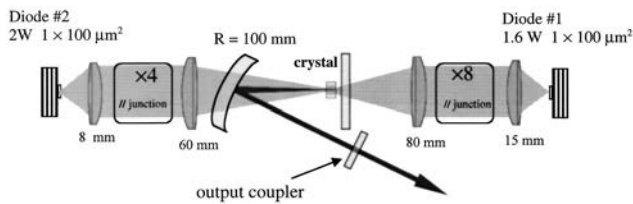


Fig. 8. Experimental setup for low-power-high-brightness pumping of Yb:BOYS. R , radius of curvature.

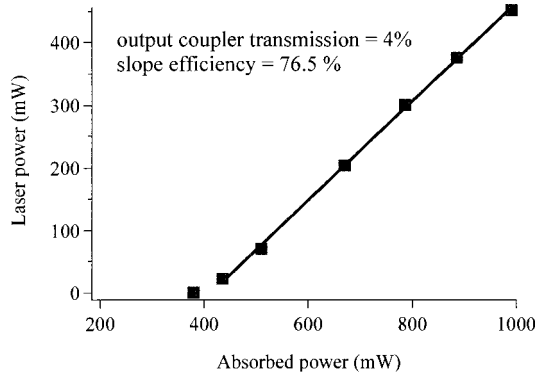


Fig. 9. Performance under low-power high-brightness pumping of Yb:BOYS with Diode #1 turned on (see Fig. 8).

6. CONCLUSION

In summary, we have reported the first efficient laser action from diode pumping of Yb:BOYS single crystals. Because of its broad and smooth emission spectrum (60 nm FWHM), this new crystal is competitive with other broadly tunable Yb-doped materials, such as Yb:glass, whose spectrum is similar, and borates [$\text{Ca}_4\text{GdO}(\text{BO}_3)_3$, $\text{Ca}_4\text{YO}(\text{BO}_3)_3$] for applications, for example, as femtosecond oscillators or near-IR tunable lasers. Moreover, its large absorption linewidth at 975 nm (6 nm FWHM) makes it particularly suited for efficient diode pumping. This new crystal offers, in addition, some advantages compared with glasses, such as better cross sections and higher thermal conductivity. We compared the efficiencies of Yb:BOYS, Yb:GdCOB, and Yb:QX phosphate glass under the same conditions and at high-power diode pumping (10 W after beam shaping). First we used a mechanical chopper to decrease the thermal load within the material, and we obtained 3.4 W of peak power with a slope efficiency of 56% with respect to the absorbed pump power under lasing conditions. Yb:BOYS was more efficient and exhibited a lower threshold than Yb:QX phosphate glass pumped under the same conditions. The efficiencies of Yb:BOYS and Yb:GdCOB were comparable. Large tunability over 50 nm (FWHM) was obtained with Yb:BOYS, with a tuning curve comparable in shape to that of glass. Thermal issues were met experimentally for pumping in the cw regime: From 5 W of incident pump power (2.2 W of absorbed power) a roll-off appeared in the efficiency curve, proving that thermal effects were detrimental to performance. In contrast, Yb:GdCOB exhibited no change in efficiency, even for cw pumping. But the thermal behavior of glass was even worse, because the laser oscillation threshold could not be reached before melting of the glass occurred.

It then appeared that a straightforward application for this new crystal would be as a laser medium for low-power femtosecond oscillators to produce ultrashort pulses, where it could be more efficient than glass and where it would be able to produce shorter pulses than all other Yb-doped crystals known so far. (In theory, 24-fs pulses could be obtained if all modes were locked within the tuning curve.) A final experiment carried out with lower-power but higher-brightness pumping allowed us to obtain 1.4 W (cw) of laser power in a diffraction-limited beam for 3.6 W of total diode pump power.

ACKNOWLEDGMENTS

Part of this research has been supported by the Centre National de la Recherche Scientifique within the framework of the research program "Groupement de Recherches Matériaux Laser (GdR LASMAT)." F. Druon acknowledges financial support of the Société des Amis de la Science for his postdoctoral research.

S. Chénaïs's e-mail address is sebastien.chenais@iota.u-psud.fr.

REFERENCES

1. D. S. Sumida, A. A. Betin, H. Bruesselbach, R. Bryen, S. Matthews, R. Reeder, and M. S. Mangir, "Diode-pumped Yb:YAG catches up with Nd:YAG," *Laser Focus World* **35**(6), 63–70 (1999).
2. C. Stewen, M. Larionov, A. Giesen, and K. Contag, "Yb:YAG thin disk laser with 1 kW output power," in *Advanced Solid State Lasers*, Vol. 34 of OSA Trends in Optics and Photonics Series (Optical Society of America, Washington, D.C., 2000), pp. 35–41.
3. P. Loosen, "Lasers in material processing," in *Advances in Lasers and Applications*, D. M. Finlayson and B. D. Sinclair, eds. (Institute of Physics Publishing, Bristol, UK, 1998), pp. 287–317.
4. S. Chénaïs, F. Druon, F. Balembois, P. Georges, A. Brun, A. Brenier, and G. Boulon, "Diode-pumped cw operation of Yb:GGG laser," in *Conference on Lasers and Electro-Optics (CLEO)*, Vol. 56 of OSA Trends in Optics and Photonics Series (Optical Society of America, Washington, D.C., 2001), pp. 170–171.
5. K. Petermann, G. Huber, L. Fornasiero, S. Kuch, E. Mix, V. Peters, and S. A. Basun, "Rare-earth-doped sesquioxides," *J. Lumin.* **87–89**, 973–975 (2000).
6. M. Larionov, A. Giesen, K. Contag, V. Peters, E. Mix, L. Fornasiero, K. Petermann, and G. Huber, "Thin disk laser operation and spectroscopic characterization of Yb-doped sesquioxides," in *Advanced Solid State Lasers*, Vol. 50 of OSA Trends in Optics and Photonics Series (Optical Society of America, Washington, D.C., 2001), paper WC4.
7. N. V. Kuleshov, A. A. Lagatsky, V. G. Shcherbitsky, V. P. Mikhailov, E. Heumann, T. Jensen, A. Dening, and G. Huber, "Cw laser performance of Yb and Er, Yb doped tungstates," *Appl. Phys. B* **64**, 409–413 (1997).
8. A. A. Lagatsky, N. V. Kuleshov, and V. P. Mikhailov, "Diode-pumped cw lasing of Yb: KYW and Yb:KGW," *Opt. Commun.* **165**, 71–75 (1999).
9. S. Erhard, J. Gao, A. Giesen, K. Contag, A. A. Lagatsky, A. Abdolvand, N. V. Kuleshov, J. Aus der Au, G. J. Spülher, F. Brunner, R. Paschotta, and U. Keller, "High power Yb:KGW and Yb:KYW thin disk laser operation," in *Conference on Lasers and Electro-Optics (CLEO)*, Vol. 56 of OSA Trends in Optics and Photonics Series (Optical Society of America, Washington, D.C., 2001), pp. 333–334.
10. P.-H. Haumesser, R. Gaumé, B. Viana, E. Antic-Fidancev, and D. Vivien, "Spectroscopic and crystal-field analysis of

- new Yb-doped laser materials,” *J. Phys. Condens. Matter* **13**, 5427–5447 (2001).
11. S. Chénais, F. Druon, F. Balembois, G. Lucas-Leclin, P. Georges, A. Brun, F. Augé, J. P. Chambaret, G. Aka, and D. Vivien, “Multiwatt, tunable, diode-pumped CW Yb: GdCOB laser,” *Appl. Phys. B* **72**, 389–393 (2001).
 12. L. Shah, Q. Ye, J. M. Eichenholz, D. A. Hammons, M. Richardson, B. H. T. Chai, and R. E. Peale, “Laser tunability in $\text{Yb}^{3+}:\text{YCa}_4\text{O}(\text{BO}_3)_3$ {Yb:YCOB},” *Opt. Commun.* **167**, 149–153 (1999).
 13. P.-H. Haumesser, R. Gaumé, J.-M. Benitez, B. Viana, B. Ferrand, G. P. Aka, and D. Vivien, “Czochralski growth of six Yb-doped double borate and silicate laser materials,” *J. Cryst. Growth* **33**, 233–242, (2001).
 14. F. Brunner, G. J. Spülher, J. Aus der Au, L. Krainer, F. Morier-Genoud, R. Paschotta, N. Lichtenstein, S. Weiss, C. Harder, A. A. Lagatsky, A. Abdolvand, N. V. Kuleshov, and U. Keller, “Diode-pumped femtosecond Yb:KGd(WO₄)₂ laser with 1.1-W average power,” *Opt. Lett.* **25**, 1119–1121 (2000).
 15. C. Hönninger, R. Paschotta, M. Graf, F. Morier-Genoud, G. Zhang, M. Moser, S. Biswal, J. Nees, A. Braun, G. A. Mourou, I. Johannsen, A. Giesen, W. Seeber, and U. Keller, “Ultrafast ytterbium-doped bulk lasers and laser amplifiers,” *Appl. Phys. B* **69**, 3–17 (1999).
 16. G. Aka, A. Kahn-Harari, F. Mougél, D. Vivien, F. Salin, P. Coquelin, P. Colin, D. Pelenc, and J. P. Damelet, “Linear and nonlinear-optical properties of a new gadolinium calcium oxoborate crystal, $\text{Ca}_4\text{GdO}(\text{BO}_3)_3$,” *J. Opt. Soc. Am. B* **14**, 9, 2238–2247 (1997).
 17. T. Danger, E. Mix, E. Heumann, G. Huber, D. Ehrt, and W. Seeber, “Diode-pumped continuous-wave Yb laser in fluoride phosphate glasses,” in *Advanced Solid State Lasers*, Vol. 1 of OSA Trends in Optics and Photonics Series (Optical Society of America, Washington, D.C., 1996), pp. 23–25.
 18. H. Liu, S. Biswal, J. Paye, J. Nees, G. Mourou, C. Hönninger, and U. Keller, “Directly diode-pumped millijoule subpicosecond Yb:glass regenerative amplifier,” *Opt. Lett.* **24**, 917–919 (1999).
 19. F. Druon, F. Balembois, P. Georges, A. Brun, A. Courjaud, C. Hönninger, F. Salin, A. Aron, F. Mougél, G. Aka, and D. Vivien, “Generation of 90-fs pulses from a mode-locked diode-pumped $\text{Yb}^{3+}:\text{Ca}_4\text{GdO}(\text{BO}_3)_3$ laser,” *Opt. Lett.* **25**, 423–425 (2000).
 20. H. Liu, J. Nees, and G. Mourou, “Diode-pumped Kerr-lens mode-locked Yb:KYW laser,” in *Conference on Lasers and Electro-Optics (CLEO)*, Vol. 56 of OSA Trends in Optics and Photonics Series (Optical Society of America, Washington, D.C., 2001), pp. 30–31.
 21. R. Gaume, P. H. Haumesser, B. Viana, G. Aka, and D. Vivien, “ Yb^{3+} lasers based on Yb doped $M_3RE(\text{BO}_3)_3$ where $M = \text{Ba}, \text{Sr}$ and $RE = \text{Lu}, \text{Y}, \text{Sc}$,” U.S. patent 09,782,787 (February 14, 2001).
 22. W. A. Clarkson, N. S. Felgate, and D. C. Hanna, “Resonator design considerations for power-scaling TEM₀₀ operation of end-pumped solid-state lasers,” in *Advanced Solid State Lasers*, Vol. 19 of OSA Trends in Optics and Photonics Series (Optical Society of America, Washington, D.C., 1998), pp. 401–406.
 23. U. Brauch, A. Giesen, M. Karszewski, Chr. Stewen, and A. Voss, “Multiwatt diode-pumped Yb:YAG thin disk laser continuously tunable between 1018 and 1053 nm,” *Opt. Lett.* **20**, 713–715 (1995).